Acta Cryst. (1967). **22**, 58

An X-ray Diffraction Analysis of Potassium Bromide

BY V. MEISALO AND O. INKINEN
Department of Physics, University of Helsinki, Helsinki, Finland

(*Received* 7 *March* 1966 *and in revised form* 10 *June* 1966)

The structure factors of potassium bromide were determined at 300°K from the integrated intensities of Bragg reflexions from powder samples. The intensities were placed on an absolute scale by the direct intensity measurement of the primary X-ray beam. Extinction, surface roughness, and preferred orientation effects were found to be negligible. The values $B_K = 2{\cdot}45 \pm 0{\cdot}15$ Å^2 and $B_{Br} = 2{\cdot}23 \pm 0{\cdot}15$ Å^2 were obtained for the temperature parameters, which correspond to the characteristic temperature $\Theta_M = 157 \pm 8$°K. The crystal radii of the ions were evaluated as $R_K = 1{\cdot}57 \pm 0{\cdot}07$ Å, and $R_{Br} = 1{\cdot}73 \pm 0{\cdot}07$ Å. The average electron density in the space outside the ionic spheres was found to be considerably low, as expected from the heteropolar character of the bonding in KBr. Deviations from spherical symmetry were revealed in the outer electron distributions of potassium and bromide ions. Both ions were shown to be compressed in the crystalline environment compared with the theoretical free ions. For the potassium ion the Hartree–Fock form factors showed a better agreement with the experimental values than those calculated from Dirac–Slater wave functions, while for the bromide ion the latter values were preferable.

Introduction

The electronic structure of alkali halide crystals has been the object of several X-ray investigations. For instance, sodium chloride has so far been studied most intensively (Witte & Wölfel, 1955; Schoknecht, 1957; Vihinen, 1960; Abrahams & Bernstein, 1965). By these investigations, a number of interesting features of the electron distribution in alkali halide crystals have been found through the structure factors determined from the integrated intensities of X-ray reflexions. Although, because of experimental limitations, such as the difficulty in obtaining higher order Fourier components, it is not possible to give a complete synthesis of the charge distribution from experimental data, one may obtain information about the outer electron distribution for each atom by comparison of the observed values for lower order components with those derived from various theories. In order to minimize the effect of series termination, one may use the usual difference series method or the Gaussian analysis (Hosemann & Bagchi, 1962). For certain details in the electron distribution of atoms, the 'non-approximate' method developed by Kurki-Suonio (1959, 1962*a*) may also be utilized.

The present study deals with the intensity measurement of X-ray reflexions from potassium bromide, which has a face-centered cubic structure with $a = 6{\cdot}602$ Å ($T = 300$°K) (Swanson & Tatge, 1953). Baldwin, Pearman & Tompson (1965) determined the X-ray characteristic temperature and the average total r.m.s. vibrational amplitude of the ions as a function of temperature. Wasastjerna (1944, 1946), using the photographic method, measured the structure factors of potassium bromide, and his data have been analyzed by Korhonen (1956). In view of the recent advances in X-ray intensity measurement, however, it seemed that a new X-ray diffraction analysis of potassium bromide might be worth carrying out. The present work gives information about the ionic form factors and the distortion in the outer electron distribution of ions in the crystalline environment. In X-ray intensity measurements with single crystals, the extinction effects may accompany the lower order reflexions which are important for distinguishing the atoms in solids and free states most clearly. The present study was therefore performed with powder samples exclusively.

Experimental

Samples

The potassium bromide used in the samples was of quality 'pro analysi' by E. Merck A.G. (Darmstadt, Germany). The major impurities were 0·1% Cl and 0·02% Na. For preliminary studies, four kinds of crystalline powder were prepared as follows:

(*a*) Large crystals formed by slow cooling from the melt were crushed and ground in an agate mortar, and then the particles were filtered through a 30-micron sieve. The powder obtained was further ground until the average particle size became of the order of 3 microns.

(*b*) The powder was prepared by rapid cooling of the melt by pouring it onto a cooled copper plate. After grinding, the particle size was found to be about 3 microns.

(*c*) A saturated aqueous solution of potassium bromide heated up to 90°C was rapidly precipitated by pouring the solution into cool absolute alcohol. The precipitate was quickly separated and dried in an electric furnace and then larger particles were removed by means of a 30-micron sieve. The average particle size was found to be somewhat smaller than 20 microns.

(*d*) The powder (*c*) was ground further until the particle size became about 2 microns.

A number of samples were prepared by pressing in a polished mould. Because the absorption coefficient of potassium bromide for Cu $K\alpha$ X-rays is relatively high, the effect of surface roughness should be avoided carefully. Comparison of the lowest-angle reflexions from samples having a different surface treatment, however, showed that the effect due to the surface roughness was negligible. The extinction effects were checked by the procedure suggested by Vand (1955). It was revealed that the integrated intensities of the reflexions 200 and 220 from the samples prepared from powder (*c*) clearly showed a diminution due to extinction effects, but the other powders proved to be extinction-free to within the accuracy of the method.

Preferred orientation was investigated by observing the variation of the integrated intensity of several reflexions with the moulding pressure ranging from that just sufficient to hold the powder in a sample vessel to about 10000 lb.in^{-2}. Preferred orientation first became noticeable at pressures exceeding 7500 lb.in^{-2}. The samples used for the final measurements were therefore moulded under pressures less than 6000 lb.in^{-2}. Orientation texture was also checked by cutting a sample in different directions relative to the direction of the compression applied, and it was proved that there was no effect of texture on the integrated intensities.

Four types of sample, referred to hereafter as samples *A*, *B*, *C* and *D*, were used for the final measurements. Samples *A*, *B* and *C* were prepared from powder (*a*), and sample *D* from powder (*d*). Their features were as follows: *A*. Moulding pressure 5000 to 6000 lb.in^{-2}. The surface layer was removed and the new surface was treated with fine emery paper. *B*. The powder was packed into a sample vessel by pressing it on a glass plate by hand. The packing was renewed several times during the measurements. *C*. Moulding pressure 3000 to 4000 lb.in^{-2}. The surface was cut off and smoothed with a razor blade and fine emery paper. *D*. Moulding pressure 300 to 500 lb.in^{-2}. The surface was cut off and smoothed with a razor blade. For samples *A*, *C* and *D*, the surface was renewed at least once during the measurements.

Measurements

The intensities of X-ray reflexions were measured with a Siemens diffractometer (Kristalloflex 4), of the X-ray beam stability within 0·3%. The detector consisted of a NaI(Tl) scintillation counter, with a linear amplifier, a differential discriminator, a ratemeter, and a recorder. The pulse-height analyser was indispensable for the measurements because of the high background caused by fluorescent radiations. The linearity of the apparatus was checked by the multiple-foil technique and the overall dead-time was found to be 2·5 μsec. The dead-time correction was applied to the integrated intensities of the strongest reflexions, and was in all cases less than 1%. Cu $K\alpha$ radiation, filtered with a nickel foil, was used in the measurements for reflexions up to 820, and Mo $K\alpha$ radiation, monochromated by a bent ground quartz crystal set in front of the detector, for reflexions from 620 up to 10, 4, 2.

The condition of symmetrical reflexion and the θ–2θ relationship between sample face and receiving slit were adjusted to 0·05° in 2θ. The general feature of the background was investigated accurately before the final measurements in order to know, for example, the influence of the *K* absorption edge of the filter on the background level. With a receiving slit of 0·4 mm, the diffraction peaks were recorded including the tails of the reflexions. The values of the relative integrated intensities were obtained by measuring, with a planimeter, the areas under the peaks above the base line corresponding to the background intensity.

On the average, five to six intensity series were recorded for each sample. The data were normalized by making the sum of the intensities equal for all different sets, and the (uncorrected) mean values of the intensities of lower-angle reflexions for each sample, the mean values for the series of samples, and the standard deviations from those means are shown in Table 1. From these data one can conclude that there are no systematic differences due to the different preparations of samples.

The integrated intensity of a Bragg reflexion from an ideal powder sample can be expressed as

$$\frac{E\omega}{I_0} = r_0^2 \frac{\lambda^3 dl}{32\pi r^2} \frac{N^2 p F^2 L}{\mu} \quad \text{(James, 1962)}, \quad (1)$$

where E is the total energy diffracted into the counter, ω the angular velocity of the counter rotation, I_0 the power of the primary beam, $r_0 = e^2/m_0c^2$ the classical electron radius, λ the X-ray wavelength, d the width of the receiving slit of height l, r the receiving slit to

Table 1. *Relative integrated intensities* (E_A, E_B, E_C, E_D), *mean values* ($\bar{E}$), *and standard deviations* ($\sigma\bar{E}$) *for lower-angle reflexions of potassium bromide measured for four types of sample*

hkl	E_A	E_B	E_C	E_D	$\bar{E}$	$\sigma\bar{E}$(%)
111	29·33	28·36	28·82	28·60	28·78	0·7
200	156·79	159·36	158·20	157·61	157·99	0·4
220	97·74	97·44	100·16	98·42	98·94	0·5
311	12·38	12·57	11·91	11·94	12·20	1·3
222	31·21	29·79	31·14	31·21	30·84	1·1
400	14·66	14·63	14·08	14·33	14·43	1·0
331	4·93	4·84	4·77	4·94	4·87	0·9
420	31·80	30·38	30·74	31·61	31·13	1·1
422	21·17	20·63	20·20	21·16	20·82	1·2

sample distance, N the number of unit cells per unit volume, p the multiplicity, μ the linear absorption coefficient, and F the structure factor. When a monochromator is used, the factor L is given by $L=(1+\cos^2 2\theta_M \cos^2 2\theta)/\sin\theta \sin 2\theta$, where θ_M is the Bragg angle of the monochromator crystal. Without a monochromator $L=(1+\cos^2 2\theta)/\sin\theta \sin 2\theta$. With the present experimental arrangement including a monochromator, we have from (1)

$$I_0=\frac{\omega r}{d}\,\frac{2E_0}{1+\cos^2 2\theta_M}, \qquad (2)$$

where E_0 is the energy diffracted from the monochromator into the counter when it is rotated through the angle $\theta=0$. Thus for the absolute structure factor one obtains from (1) and (2)

$$F^2(hkl)=\left(\frac{4}{Nr_0}\right)^2 \frac{\pi r\mu(1+\cos^2 2\theta_M)}{\lambda^3 lLp}\,\frac{E(hkl)}{E_0}. \qquad (3)$$

The main difficulties in the absolute standardization of the data were due to the high value of μ and the necessity of reducing the primary beam intensity by an accurately known factor of about 100. Because it was difficult to measure the absorption coefficient directly, we adopted the tabulated value $\mu=313$ cm^{-1} (Cu $K\alpha$) (*International Tables for X-ray Crystallography*, 1962). The reduction of the primary beam was accomplished by nickel absorbers of various thicknesses. The attenuation factors of these were determined with the use of single-crystal (potassium bromide) reflexion.

Among the powder reflexions, only the 200 and 220 lines were strong enough to give sufficiently accurate values for E/E_0. By combining the results of the relative structure factor measurements with the measured absolute values of $F_o(200)$ and $F_o(220)$, the final absolute structure factor data were derived. Sample B was found to give about 5% lower values for E/E_0 than the other samples, probably because of its porosity (Harrison & Paskin, 1964). The scale factor was therefore determined as a mean of the values obtained with samples A, C and D, which are in agreement with one another within 1%. The uncertainty of the scale factor was estimated to be about 1·5%, not including the possible error in μ.

The structure factors

For potassium bromide the structure factors are expressed, in terms of the scattering factors of the ions, f_K and f_{Br}, by

$$F(hkl)=4[f_{Br}\exp(-M_{Br})\pm f_K\exp(-M_K)], \qquad (4)$$

where the plus sign applies to all even h, k, l, and the minus sign to all odd. The expression $\exp(-M)$ is the Debye–Waller temperature factor, with $M=B(\sin^2\theta)/\lambda^2$. The theoretical structure factors were computed from the Hartree–Fock (HF) form factors calculated by Freeman (1959) for free K^+, and those by Freeman & Watson (*International Tables*, 1962) for free Br^-. For comparison we also used the values computed by Cromer & Waber (1965) with the relativistic Dirac–Slater (DS) wave functions. These values differ from HF data but are in good agreement with those calculated by Hanson, Herman, Lea & Skillman (1964) from Hartree–Fock–Slater wave functions. To obtain interpolated values of the theoretical form factors for each hkl, the Gaussian representation

$$f=\sum_i a_i \exp[-b_i(\sin^2\theta)/\lambda^2] \qquad (5)$$

was used for the HF values, with the parameters a_i and b_i determined by Kurki-Suonio, Meisalo, Merisalo & Peltola (1966). This gave a satisfactory fit to the tabulated values. For the dispersion terms $\Delta f'$ and $\Delta f''$ of each ion, we used the values calculated by Cromer (1965).

The temperature parameters of the individual ions were determined by using the criterion of minimum curvature of the $\Delta\varrho$ curve at the center of the ions, where $\Delta\varrho$ is given by the Fourier difference series

$$\Delta\varrho=\varrho_o-\varrho_c=\frac{1}{V}\sum_{hkl}[F_o(hkl)-F_c(hkl)]\cos 2\pi(hx+ky+lz). \qquad (6)$$

Curve I in Fig. 1 represents the series (6) calculated along the edge of the unit cell, using the HF values, the experimental scale factor, and the temperature parameters $B_K=2{\cdot}35$ Å^2, $B_{Br}=2{\cdot}13$ Å^2. Curve II was obtained with a scale factor lower by 2%, and with the B values correspondingly adjusted to $B_K=2{\cdot}39$ Å^2, $B_{Br}=2{\cdot}17$ Å^2. The comparison of curves I and II shows the sensitivity of $\Delta\varrho$ to changes of the scale factor.

Curve III was obtained with the DS values, the experimental scale, and $B_K=2{\cdot}38$ Å^2, $B_{Br}=2{\cdot}17$ Å^2. This curve, when compared with curve I, indicates the difference corresponding to the use of different theoretical scattering factors. Curve IV shows the effect of the alterations $\Delta B_K=0{\cdot}01$ Å^2, $\Delta B_{Br}=0{\cdot}005$ Å^2 on curve I, and it demonstrates the sensitivity of $\Delta\varrho$ to changes in thermal parameters.

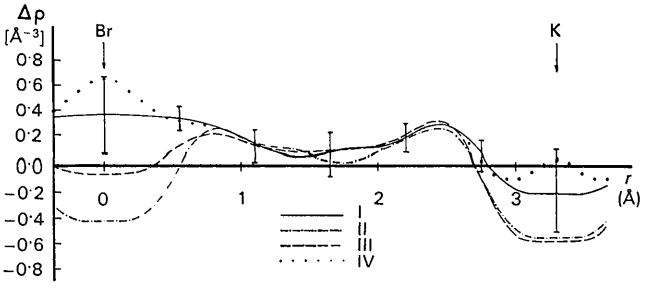

Fig. 1. Fourier difference series calculated along the edge of the unit cell (Br^- at the origin): with experimental scale factor and temperature parameters $B_K=2{\cdot}35$ Å^2, $B_{Br}=2{\cdot}13$ Å^2 (curve I); with a 2% lower scale and $B_K=2{\cdot}39$ Å^2, $B_{Br}=2{\cdot}17$ Å^2 (curve II); with experimental scale and using the DS ionic form factors with $B_K=2{\cdot}38$ Å^2, $B_{Br}=2{\cdot}17$ Å^2 curve III). Curve IV shows the effect of the alterations $\Delta B_K=0{\cdot}01$ Å^2, $\Delta B_{Br}=0{\cdot}005$ Å^2 on curve I.

The $\Delta\varrho$ curves also give a criterion concerning the scale factor (*cf.* Kurki-Suonio & Fontell, 1963). The optimum scale factor (with the optimum thermal parameters) may be obtained when the $\Delta\varrho$ curve at the ion sites is as flat as possible. The validity of this criterion, however, depends on the reliability of the theoretical ionic form factors at high values of $(\sin\theta)/\lambda$, which is not always obvious for ions as heavy as K^+ and Br^-.

From curves I, II and III we see, however, that the optimum scale is satisfactorily close to the experimental one, even for both theoretical models. We can conclude therefore that the theoretical atomic scattering factors are reliable at high values of $(\sin\theta)/\lambda$, *i.e.*, with respect to the inner electron shells, the theoretical models are fairly good.

Table 2. *Experimental dispersion-corrected structure factors F_o of* KBr *at* 300°K, *their experimental errors δF_o, theoretical structure factors F_c calculated from Hartree–Fock free-ion form factors with temperature parameters* $B_K = 2{\cdot}35$ Å^2, $B_{Br} = 2{\cdot}13$ Å^2, *and the differences* $\Delta F = F_o - F_c$

The values are for a molecular unit of KBr. Overlapping reflexions combined by curly brackets have been divided in the theoretical ratio.

h k l	sinθ/λ (Å⁻¹)	F_o	δF_o	F_c	ΔF
1 1 1	0.1312	15.25	0.09	14.79	0.46
2 0 0	0.1515	44.58	0.19	43.06	1.52
2 2 0	0.2142	36.74	0.08	36.45	0.29
3 1 1	0.2512	11.99	0.06	11.74	0.25
2 2 2	0.2624	31.80	0.15	31.79	0.01
4 0 0	0.3029	29.10	0.15	28.23	0.87
3 3 1	0.3301	10.49	0.06	10.12	0.37
4 2 0	0.3387	25.18	0.09	25.38	-0.20
4 2 2	0.3710	22.92	0.05	23.01	-0.09
{5 1 1}	0.3935	8.83	0.05	8.91	0.08
{3 3 3}	0.3935	8.83	0.05	8.91	0.08
4 4 0	0.4284	19.06	0.12	19.19	-0.13
5 3 1	0.4481	7.60	0.06	7.53	0.07
{6 0 0}	0.4544	17.40	0.10	17.62	-0.22
{4 4 2}	0.4544	17.40	0.10	17.62	-0.22
6 2 0	0.4790	16.35	0.11	16.23	0.12
5 3 3	0.4966	6.51	0.07	6.44	0.07
6 2 2	0.5024	14.97	0.08	14.98	-0.01
4 4 4	0.5247	13.86	0.12	13.84	0.02
{7 1 1}	0.5409	5.59	0.05	5.49	0.10
{5 5 1}	0.5409	5.59	0.05	5.49	0.10
6 4 0	0.5461	12.73	0.06	12.81	-0.08
6 4 2	0.5667	11.85	0.08	11.87	-0.02
{5 5 3}	0.5817	4.55	0.03	4.69	-0.14
{7 3 1}	0.5817	4.55	0.03	4.69	-0.14
8 0 0	0.6059	10.15	0.11	10.21	-0.06
{7 3 3}	0.6199	4.11	0.06	4.13	-0.02
{6 4 4}	0.6245	9.32	0.06	9.48	-0.16
{8 2 0}	0.6245	9.32	0.06	9.48	-0.16
{6 6 0}	0.6426	8.85	0.22	8.81	0.04
{8 2 2}	0.6426	8.85	0.22	8.81	0.04
{5 5 5}	0.6559	3.37	0.06	3.42	-0.05
{7 5 1}	0.6559	3.37	0.06	3.42	-0.05
{6 6 2}	0.6602	8.06	0.19	8.20	-0.14
8 4 0	0.6774	7.97	0.25	7.79	0.18
{7 5 3}	0.6900	2.92	0.04	2.93	-0.01
{9 1 1}	0.6900	2.92	0.04	2.93	-0.01
{8 4 2}	0.6941	7.02	0.16	7.10	-0.08
6 6 4	0.7105	6.64	0.21	6.61	0.03
9 3 1	0.7225	2.43	0.09	2.52	-0.09
8 4 4	0.7420	5.64	0.18	5.74	-0.10
{7 5 5}	0.7536	2.16	0.04	2.17	-0.01
{7 7 1}	0.7536	2.16	0.04	2.17	-0.01
{9 3 3}	0.7536	2.16	0.04	2.17	-0.01
{8 6 0}	0.7573	5.28	0.13	5.35	-0.07
{10 0 0}	0.7573	5.28	0.13	5.35	-0.07
{8 6 2}	0.7723	5.11	0.16	4.99	0.12
{10 2 0}	0.7723	5.11	0.16	4.99	0.12
{7 7 3}	0.7834	1.86	0.04	1.88	-0.02
{9 5 1}	0.7834	1.86	0.04	1.88	-0.02
{6 6 6}	0.7871	4.59	0.09	4.66	-0.07
{10 2 2}	0.7871	4.59	0.09	4.66	-0.07
{9 5 3}	0.8122	1.65	0.03	1.63	0.02
{8 6 4}	0.8157	4.08	0.09	4.06	0.02
{10 4 0}	0.8157	4.08	0.09	4.06	0.02
10 4 2	0.8296	3.76	0.10	3.79	-0.03

The series (6) computed along the face diagonal and along the diagonal of the unit cell gave the same conclusions as above.

In subsequent analysis we used the parameters for curve I. The dispersion-corrected values of experimental structure factors F_o thus obtained are given in Table 2, together with the theoretical HF values F_c and the differences $\Delta F = F_o - F_c$. The δF_o values represent the estimated total errors of the relative structure factors.

Analysis and discussion

Thermal data

Experimentally obtained B values may be influenced by the contribution of thermal diffuse scattering (TDS) below the Bragg reflexions. We followed the method of Chipman & Paskin (1959), and the correction for TDS in the B values was found to be about $+0{\cdot}1$ Å^2. This resulted in the estimations $B_K = 2{\cdot}45 \pm 0{\cdot}15$ Å^2, $B_{Br} = 2{\cdot}23 \pm 0{\cdot}15$ Å^2. The value of the characteristic temperature corresponding to these data is $\Theta_M = 157 \pm 8$°K according to the relation

$$\bar{B} = \frac{6h^2}{mk\Theta_M}\left[\frac{\Phi(x)}{x} + \frac{1}{4}\right] \text{ (James, 1962),}$$

where $\bar{B}$ is the average temperature parameter, being the mean of the individual B values weighted with the atomic mass, h Planck's constant, k Boltzmann's constant and m the average mass of the ions, $x = \Theta_M/T$, with T the absolute temperature, and $\Phi(x)$ the Debye function. In the present case, $\bar{B} = 2{\cdot}30 \pm 0{\cdot}15$ Å^2.

A summary of the experimental and calculated values of B_K, B_{Br} and Θ_M is given in Table 3. Our X-ray data are in agreement with the calculated values and those obtained in previous diffraction experiments within their combined uncertainties. However, it is to be noted that both our own and Wasastjerna's X-ray data indicate that $B_K > B_{Br}$, whereas the theoretical values and those obtained in neutron diffraction experiments suggest $B_K < B_{Br}$. It is probable that the B values for X-ray scattering may differ from those for the neutron data (*cf.* Raichenko, 1965).

Crystal radii and the number of electrons in each ion

From the following analysis, we obtained the ionic scattering factor f_o corresponding to the structure amplitude for the electron distribution contained within a sphere around the ion's centre with a radius equal to the crystal radius R of the ion. The scattering factor f_o is given by the series

$$f_o(hkl) = \frac{1}{V}\sum_{h'k'l'} F_o(h'k'l')\,\sigma(h-h', k-k', l-l')\,, \qquad (7)$$

where σ is the shape transform of the sphere (for details, see Kurki-Suonio, 1959). For a cubic unit cell, we have

$$\sigma(hkl) = 4\pi R^3(\sin q - q\cos q)/q^3\,,$$

where $q = 2\pi R/d$, d being the spacing of the lattice planes (hkl).

The number of electrons belonging to K or Br ion is given from the series (7) at $(\sin\theta)/\lambda=0$ for the spheres of different size. The zero order term $F(000)$ was put equal to 54·00. For evaluation of the residual term we made use of the analytic form (5). In order to investigate the convergence of the series $f(000)$, the partial sum for a K-centred sphere with $R_K=1{\cdot}57$ Å has been calculated as a function of the cut-off limit $(\sin\theta)/\lambda$. Fig. 2 shows that the limiting value of the series can be determined rather accurately if the summation is extended to $(\sin\theta)/\lambda \gtrsim 1{\cdot}8$ Å^{-1}. The value of $f(000)$ was found to be insensitive to the choice of the Debye–Waller factors.

Table 4 gives the results obtained, where the radii R_K and R_{Br} of the spheres are chosen pairwise so as to fulfil the sum relation $R_K+R_{Br}=3{\cdot}30$ Å corresponding to the interionic distance. The average electron density $\bar{\varrho}$ outside the ionic spheres is found to be rather low, corresponding to the heteropolar character of the bonding in KBr. The values of $\bar{\varrho}$ in this space are almost equal for the last four pairs, while the value for the first two is definitely larger than those for the others. In this respect, any choice of the crystal radii between the third and the sixth pair would be equally reasonable. The slightly negative values of ϱ are of about the same order as the experimental errors. Incidentally, a scale factor higher by only about 2% was proved to be clearly unreasonable since it gave significantly negative values for $\bar{\varrho}$ in the space outside the spheres.

A natural definition of the crystal radii may be given on the basis of the values in Table 4, by finding out the point where the average electron densities for K- and Br-centred shells are equal to each other (*cf.* Kurki-Suonio & Fontell, 1964). This point is found to lie at a distance of 1·73 Å from the centre of the Br ion. By taking account of the uncertainty in the scale factor and the standard deviations calculated from experimen-

Table 4. *The number of electrons $f(000)$ and the average electron density ϱ (e.Å^{-3}) in different regions*

Region	$f(000)$	$\bar{\rho}$
K-centred sphere		
1. $R=1{\cdot}23$ Å	17·78	
2. $R=1{\cdot}33$	18·04	
3. $R=1{\cdot}41$	18·19	
4. $R=1{\cdot}49$	18·33	
5. $R=1{\cdot}56$	18·44	
6. $R=1{\cdot}67$	18·58	
Br-centred sphere		
1. $R=2{\cdot}07$ Å	36·19	
2. $R=1{\cdot}97$	36·04	
3. $R=1{\cdot}89$	35·96	
4. $R=1{\cdot}81$	35·88	
5. $R=1{\cdot}74$	35·81	
6. $R=1{\cdot}63$	35·61	
K-centred shell		
2.−1.	0·26	0·13
3.−2.	0·15	0·08
4.−3.	0·14	0·06
5.−4.	0·11	0·05
6.−5.	0·15	0·04
Br-centred shell		
1.−2.	0·16	0·03
2.−3.	0·08	0·02
3.−4.	0·08	0·02
4.−5.	0·08	0·03
5.−6.	0·20	0·05
¼ unit cell excepting the volume of a pair of spheres		
pair 1.	0·09	0·002
pair 2.	−0·07	−0·002
pair 3.	−0·15	−0·005
pair 4.	−0·21	−0·006
pair 5.	−0·24	−0·007
pair 6.	−0·19	−0·006

Table 3. *Experimental and calculated values of the temperature parameters B_K and B_{Br} (Å^2), and the Debye temperature Θ_M (°K) for* KBr *at* 300 °K

B_K	B_{Br}	Θ_M	Reference
2·45 ± 0·15	2·23 ± 0·15	157 ± 8	Present work
2·06	1·92		Observed – polycrystal X-ray (Wasastjerna, 1944)*
2·20 ± 0·10	2·28 ± 0·10		Observed – single-crystal neutron (Pryor, 1966)
2·17 ± 0·30	2·67 ± 0·30		Observed – polycrystal neutron (Pryor, 1966)
		163	Observed – polycrystal X-ray (Baldwin *et al.*, 1965)
2·01	2·13		Calc. by Raichenko (1963)
2·29	2·35	158	Calc. by Pryor (1966) from 90 °K dispersion curves and formulae of Woods *et al.* (1960, 1963) and Cowley *et al.* (1963)
2·21	2·49	156	Calc. by Pryor (1966) from 400 °K dispersion curves and formulae of Woods *et al.* (1960, 1963) and Cowley *et al.* (1963)
2·26	2·55	154	Calc. by Pryor (1966) from 300 °K physical constants
		164	Calc. by Baldwin *et al.* (1965) from the frequency spectra of Cowley *et al.* (1963)
		168	Calc. by Baldwin *et al.* (1965) from the frequency spectra of Karo & Hardy (1963)
		160	Derived by Pryor (1966) from the specific heat data of Barron *et al.* (1957)

* These values have not been corrected for TDS.

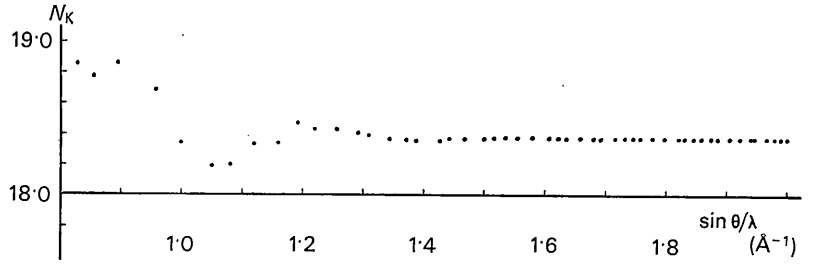

Fig. 2. Convergence of the series $f(000)$ for a K-centred sphere with radius $R = 1{\cdot}57$ Å.

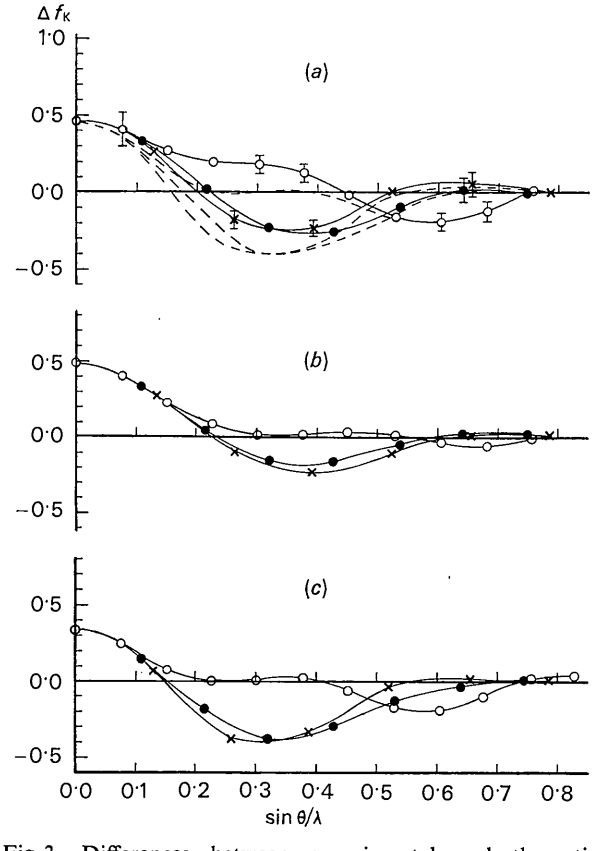

Fig. 3. Differences between experimental and theoretical structure amplitudes for a K-centred sphere with $R = 1{\cdot}57$ Å [(*a*) and (*c*)], and $R = 1{\cdot}34$ Å (*b*) in the crystallographic directions [*h*00] (circles), [*hh*0] (solid circles) and [*hhh*] (crosses). The solid and broken curves in (*a*) were obtained with the HF and DS ionic form factors, respectively. (*c*) was obtained with a scale factor lower by 2 %.

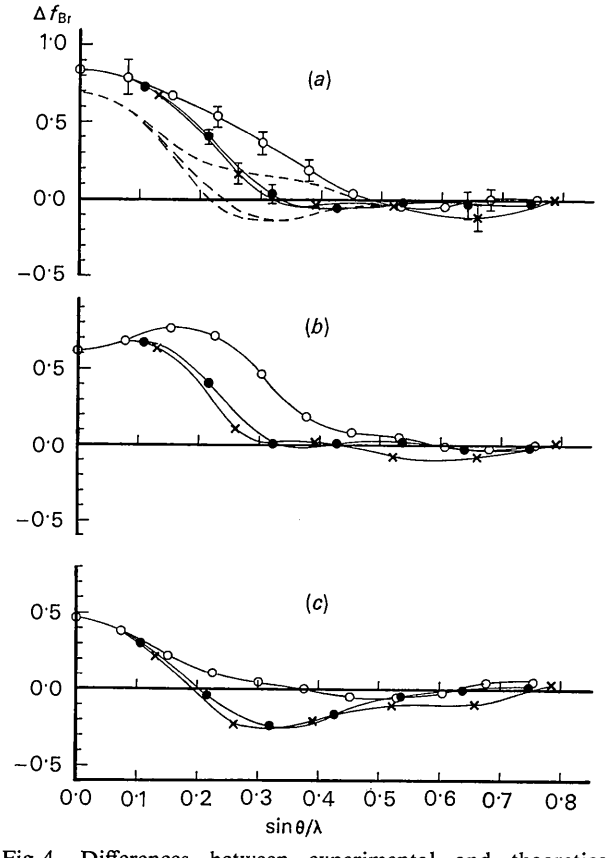

Fig. 4. Differences between experimental and theoretical structure amplitudes for a Br-centred sphere with $R = 1{\cdot}73$ Å [(*a*) and (*c*)], and $R = 1{\cdot}96$ Å (*b*). The symbols are the same as those in Fig. 3. The solid and broken curves in (*a*) were obtained with the HF and DS ionic form factors, respectively. (*c*) was obtained with a scale factor lower by 2 %.

tal errors, we obtained the estimates $R_K = 1{\cdot}57 \pm 0{\cdot}07$ Å, $R_{Br} = 1{\cdot}73 \pm 0{\cdot}07$ Å. These values are in good agreement with the crystal radii $R_K = 1{\cdot}55$ Å, $R_{Br} = 1{\cdot}75$ Å calculated by Fumi & Tosi (1964*b*) using the generalized Huggins–Mayer form for the repulsion energy, but differ remarkably from the traditional ionic and atomic radii (*cf.* Fumi & Tosi, 1964*a*; Slater, 1964). The K- and Br-centred spheres with the above crystal radii contain $18{\cdot}4 \pm 0{\cdot}2$ and $35{\cdot}8 \pm 0{\cdot}4$ electrons, respectively. The numbers of electrons in the same regions calculated on the basis of the theoretical Hartree–Fock free ions were found to be 18·0 and 35·0.

Outer electron distributions

The outer electron distributions of the ions were studied in terms of the differences appearing between the experimental and theoretical form factors of K^+ and Br^-. The calculations were made by using the series (7) with the coefficients ΔF given in Table 2, for the crystal radii obtained above and also for the tradi-

tional values $R_K = 1{\cdot}34$ Å and $R_{Br} = 1{\cdot}96$ Å. Figs. 3 and 4 show the values of Δf_K and Δf_{Br} for three main directions [*h*00], [*hh*0] and [*hhh*]. The solid and broken curves were obtained with the HF and DS form factors respectively. Figs. 3(*c*) and 4(*c*) show the results obtained with a scale factor lower by 2% and with temperature factors corresponding to curve II in Fig. 1. The error marks at a few points in Figs. 3(*a*) and 4(*a*) indicate the standard deviations calculated from experimental errors.

Figs. 3 and 4 show that both Δf_K and Δf_{Br} curves for different directions are accompanied by significant anisotropy at small values of $(\sin\theta)/\lambda$, implying non-spherical deformations in the outer electron distribution of the ions. The differences are almost independent of the scale factor, the temperature factors, and the choice of theoretical form factors. Concerning the significance of the observed anisotropy, the errors arising from possible preferred orientation of particles in the samples may be most critical. However, it was proved that all data of Δf_K and Δf_{Br} calculated with the F_o values obtained from integrated intensities of various samples (see Table 1) gave essentially the same result within the standard deviations. It is to be noted that Korhonen's (1956) analysis of the structure factors of potassium bromide measured by Wasastjerna (1944) has led to results similar to ours.

From the general behaviour of the Δf_K and Δf_{Br} curves we can infer some qualitative features of the non-spherical deformations. If we take the average of the curves for different directions as a reference, our results show that both the potassium and bromide ions are compressed in the [*h*00] direction along which the ions are closest to each other. In the [*hh*0] and [*hhh*] directions, on the other hand, an expansion of the electron distribution of the ions takes place. These features are physically natural, and are similar to the results found for several other ionic crystals (Korhonen, 1956; Kurki-Suonio & Fontell, 1964; Inkinen & Meisalo, 1965; Kurki-Suonio & Meisalo, 1966; Merisalo & Inkinen, 1966). Comparison of Figs. 3(*a*) and 3(*b*) indicates that for the potassium ion the non-spherical deformation takes place almost exclusively in parts outside the traditional ionic radius. This appears to be reasonable since the charge clouds contributed by the outer shell electrons would be most easily deformed. It should be noted, however, that the observed anisotropy may include the effect of anisotropic lattice vibrations too.

The general trend of the Δf_K and Δf_{Br} curves shows that the experimental scattering factors are larger than the theoretical ones at small values of $(\sin\theta)/\lambda$, thus indicating that each ion is compressed as a whole in the crystalline environment compared with the free ion states. This fact is also in accordance with the 2% excess of electrons observed in the regions of the K and Br ions (see above under *Crystal radii and the number of electrons in each ion*). The magnitude of the deviations depends on the choice of the theoretical form factors. For the potassium ion the HF form factors agree better with the experimental values than those from DS wave functions, but for the heavier bromide ion the latter values are preferable. This is reasonable because, in the DS model, the relativistic effect (which is trivial for lighter elements), and also at least approximately the exchange effect, have been taken into account.

Estimation of the extent of the average spherical compression of the ions is influenced by the uncertainty of about 2% in the scale factor. However, it is interesting to note that similar compressions have been measured also in other ionic crystals (*e.g.* Calder, Cochran, Griffiths & Lowde, 1962; Kurki-Suonio & Fontell, 1964; Inkinen & Meisalo, 1965; Merisalo & Inkinen, 1966), and have also been concluded in theoretical studies taking account of the effect of the crystalline field (*e.g.* Hurst, 1959; Mansikka, 1965).

We wish to thank Prof. P. E. Tahvonen for his interest in our work and Dr K. Kurki-Suonio for valuable discussions. We are also indebted to Mr L. Fontell, Phil. Mag., for the programming work, and to Mrs Lorna Sundström, M.Sc., for revising the English of the manuscript.

This research has been financially supported by the Finnish Atomic Energy Commission (V.M.) and the National Research Council for Sciences, Finland (O.I.).

References

Abrahams, S. C. & Bernstein, J. L. (1965). *Acta Cryst.* **18**, 926.

Baldwin, T. O., Pearman, G. T. & Tompson, C. W. (1965). *J. Phys. Chem. Solids*, **26**, 303.

Barron, T. H. K., Berg, W. T. & Morrison, J. A. (1957). *Proc. Roy. Soc.* A, **242**, 478.

Calder, R. S., Cochran, W., Griffiths, D. & Lowde, R. D. (1962). *J. Phys. Chem. Solids*, **23**, 621.

Chipman, D. R. & Paskin, A. (1959). *J. Appl. Phys.* **30**, 1992.

Cowley, R. A., Cochran, W., Brockhouse, B. N. & Woods, A. D. B. (1963). *Phys. Rev.* **131**, 1030.

Cromer, D. T. (1965*a*). *Acta Cryst.* **18**, 17.

Cromer, D. T. (1965*b*). *Acta Cryst.* **19**, 224.

Cromer, D. T. & Waber, J. T. (1965). *Acta Cryst.* **18**, 104.

Freeman, A. J. (1959). *Acta Cryst.* **12**, 261.

Freeman, A. J. & Watson, R. E. (1962). In *International Tables for X-ray Crystallography*, Vol. III, Table 3.3.1A. Birmingham: Kynoch Press.

Fumi, F. G. & Tosi, M. P. (1964*a*). *J. Phys. Chem. Solids*, **25**, 31.

Fumi, F. G. & Tosi, M. P. (1964*b*). *J. Phys. Chem. Solids*, **25**, 45.

Hanson, H. P., Herman, F., Lea, J. D. & Skillman, S. (1964). *Acta Cryst.* **17**, 1040.

Harrison, R. J. & Paskin, A. (1964). *Acta Cryst.* **17**, 325.

Hosemann, R. & Bagchi, S. N. (1962). *Direct Analysis of Diffraction by Matter*. Amsterdam: North-Holland Publishing Co.

Hurst, R. P. (1959). *Phys. Rev.* **114**, 746.

Inkinen, O. & Meisalo, V. (1965). *J. Phys. Soc., Japan*, **20**, 2101.

International Tables for X-ray Crystallography (1962). Vol. III, Table 3.2.2.A. Birmingham: Kynoch Press.
JAMES, R. W. (1962). *The Optical Principles of the Diffraction of X-rays*, p. 51. London: Bell.
KARO, A. M. & HARDY, J. R. (1963). *Phys. Rev.* **129**, 2024.
KORHONEN, U. (1956). *Ann. Acad. Sci. Fenn.* A.I, No. 221.
KURKI-SUONIO, K. (1959). *Ann. Acad. Sci. Fenn.* A.VI, No. 31.
KURKI-SUONIO, K. (1962*a*). *Ann. Acad. Sci. Fenn.* A.VI, No. 93.
KURKI-SUONIO, K. (1962*b*). *Ann. Acad. Sci. Fenn.* A.VI, No. 94.
KURKI-SUONIO, K. & FONTELL, L. (1963). *Ann. Acad. Sci. Fenn.* A.VI, No. 135.
KURKI-SUONIO, K. & FONTELL, L. (1964). *Ann. Acad. Sci. Fenn.* A.VI, No. 161.
KURKI-SUONIO, K. & MEISALO, V. (1966). *J. Phys. Soc., Japan*, **21**, 122.
KURKI-SUONIO, K., MEISALO, V., MERISALO, M. & PELTOLA, E. (1966). *Ann. Acad. Sci. Fenn.* A.VI, No. 198.
MANSIKKA, K. (1965). Private communication.
MERISALO, M. & INKINEN, O. (1966). *Ann. Acad. Sci. Fenn.* A.VI, No. 207.
PRYOR, A. W. (1966). *Acta Cryst.* **20**, 138.
RAICHENKO, A. I. (1963). *Fizika Tverdogo Tela*, **5**, 1982.
RAICHENKO, A. I. (1965). *Fizika Tverdogo Tela*, **7**, 877.
SCHOKNECHT, G. (1957). *Z. Naturforsch.* **12**a, 983.
SLATER, J. C. (1964). *J. Chem. Phys.* **41**, 3199.
SWANSON, H. E. & TATGE, E. (1953). NBS Circular No. 539.
VAND, V. (1955). *J. Appl. Phys.* **26**, 1191.
VIHINEN, S. (1960). *Ann. Acad. Sci. Fenn.* A.VI, No. 52.
WASASTJERNA, J. A. (1944). *Acta Soc. Sci. Fenn.* A.III, No. 6.
WASASTJERNA, J. A. (1946). *Soc. Sci. Fenn. Comm. Phys.-Math.* XIII, No. 5.
WITTE, H. & WÖLFEL, E. (1955). *Z. phys. Chem.*, Neue Folge **3**, 296.
WOODS, A. D. B., BROCKHOUSE, B. N. & COWLEY, R. A. (1963). *Phys. Rev.* **131**, 1025.
WOODS, A. D. B., COCHRAN, W. & BROCKHOUSE, B. N. (1960). *Phys. Rev.* **119**, 980.

Acta Cryst. (1967). **22**, 65

Three-Dimensional X-ray Analysis of the Complex $CaBr_2.10H_2O.2(CH_2)_6N_4$

BY L. MAZZARELLA, A. L. KOVACS, P. DE SANTIS AND A. M. LIQUORI

Istituto Chimico, Centro Nazionale di Chimica delle Macromolecole (CNR), Sez. III, *Via Mezzocannone* 4, *Napoli, Italy*

(*Received* 25 *April* 1966)

Crystals of the complex $CaBr_2.10H_2O.2(CH_2)_6H_4$ are triclinic, space group $P\bar{1}$, with $a=9{\cdot}89\pm0{\cdot}02$, $b=9{\cdot}75\pm0{\cdot}02$, $c=9{\cdot}58\pm0{\cdot}02$, $\alpha=94°29'\pm12'$, $\beta=100°39'\pm12'$, $\gamma=119°20'\pm12'$, $Z=1$. The crystal structure has been determined by the heavy-atom method and then refined by three-dimensional Fourier synthesis and several cycles of differential synthesis. The structure is characterized by layers parallel to (001), in which each hexamethylentetramine molecule links three different $Ca(H_2O)_6^{2+}$ octahedra and each $Ca(H_2O)_6^{2+}$ octahedron links six different hexamethylenetetramine molecules. The structure is fully hydrogen bonded.

Introduction

The problem of solvation of biological macromolecules in aqueous solutions has become extremely interesting within the past few years and an increasing number of studies on simple models have been carried out.

It appeared of some interest to us to clarify some structural aspects of complexes between organic bases and inorganic salts in which high forms of hydration are often stabilized. Hexamethylenetetramine (HMT) forms a large series of complexes with different inorganic salts, linking also a high number of water molecules (Table 1). These complexes were first crystallized by Barbieri & Calzolari (1910). Bertinotti & Liquori (1953) investigated the structure of the complex $CaBr_2.10H_2O.2$(HMT) and of the corresponding magnesium chloride complex by two-dimensional X-ray analysis. However, the many superpositions of atoms made it impossible to unravel the structures completely. It was therefore decided to carry out a three-dimensional analysis of the complex $CaBr_2.10H_2O.2$(HMT) and to examine the relationship between this structure and that of a cubic modification studied by Addamiano & Giacomello (1951). Some preliminary results have already been reported (De Santis, Kovacs, Liquori & Mazzarella, 1965).

Table 1. *Some complexes between hexamethylenetetramine and inorganic salts*

General formula	A
A . $10H_2O$. 2(HMT)	$CaBr_2$, $MgCl_2$, $MnCl_2$, $CoCl_2$, $NiCl_2$, $MnBr_2$, $MgBr_2$, $CoBr_2$, $NiBr_2$, NiI_2, CoI_2, MnI_2, MgI_2, $Mg(SCN)_2$, $Mg(NO_3)_2$, $Co(NO_3)_2$, $Mn(NO_3)_2$, $Y(NO_3)_3$.
A . $8H_2O$. 2(HMT)	$Mg(ClO_4)_2$, $Co(ClO_4)_2$, $Ni(ClO_4)_2$.
A . $7H_2O$. 2(HMT)	$MnCr_2O_7$, $MgCr_2O_7$.